# MindFormer: A Transformer Architecture for Multi-Subject Brain Decoding via fMRI

Inhwa Han Jaayeon Lee Jong Chul Ye
Kim Jaechul Graduate School of AI
Korea Advanced Institute of Science and Technology (KAIST), Daejeon, Korea
{inhwahan, jaayeon, jong.ye}@kaist.ac.kr

### **Abstract**

Research efforts to understand neural signals have been ongoing for many years, with visual decoding from fMRI signals attracting considerable attention. Particularly, the advent of image diffusion models has advanced the reconstruction of images from fMRI data significantly. However, existing approaches often introduce inter- and intra- subject variations in the reconstructed images, which can compromise accuracy. To address current limitations in multi-subject brain decoding, we introduce a new Transformer architecture called *MindFormer*. This model is specifically designed to generate fMRI-conditioned feature vectors that can be used for conditioning Stable Diffusion model. More specifically, MindFormer incorporates two key innovations: 1) a novel training strategy based on the IP-Adapter to extract semantically meaningful features from fMRI signals, and 2) a subject specific token and linear layer that effectively capture individual differences in fMRI signals while synergistically combines multi subject fMRI data for training. Our experimental results demonstrate that Stable Diffusion, when integrated with MindFormer, produces semantically consistent images across different subjects. This capability significantly surpasses existing models in multi-subject brain decoding. Such advancements not only improve the accuracy of our reconstructions but also deepen our understanding of neural processing variations among individuals.

### 1 Introduction

Brain decoding is the field focused on interpreting neural activity patterns to understand cognitive and sensory processes [1–6]. Utilizing neuroimaging techniques such as functional magnetic resonance imaging (fMRI), researchers measure neural responses of brain activity to cognitive and sensory stimuli. Especially, visual brain decoding is a rapidly advancing field that aims to interpret brain activity to reconstruct visual experiences. Since the advent of deep learning, this field has significantly advanced [7–12]. One popular approach to visual decoding involves mapping brain activity to latent spaces of generative models, such as generative adversarial networks (GANs) [13–16]. With new large-scale fMRI datasets [17], recent advancements have also seen the use of diffusion models to improve reconstruction accuracy [18–25]. The integration of diffusion models in brain decoding represents a significant leap forward, providing sophisticated tools to reconstruct and understand complex neural representations. However, challenges remain in achieving high fidelity, lightweight model and integrated-subject brain decoding.

In this work, we introduce a unified transformer architecture named MindFormer, which demonstrates exceptional performance in multi-subject brain decoding. MindFormer is specifically designed to generate semantically meaningful feature embeddings that facilitate fMRI-conditioned image generation using the Stable Diffusion model. We utilize the IP-adapter, as described in [26], to generate 16x768-dimensional feature embeddings from fMRI signals, which serve as conditions for

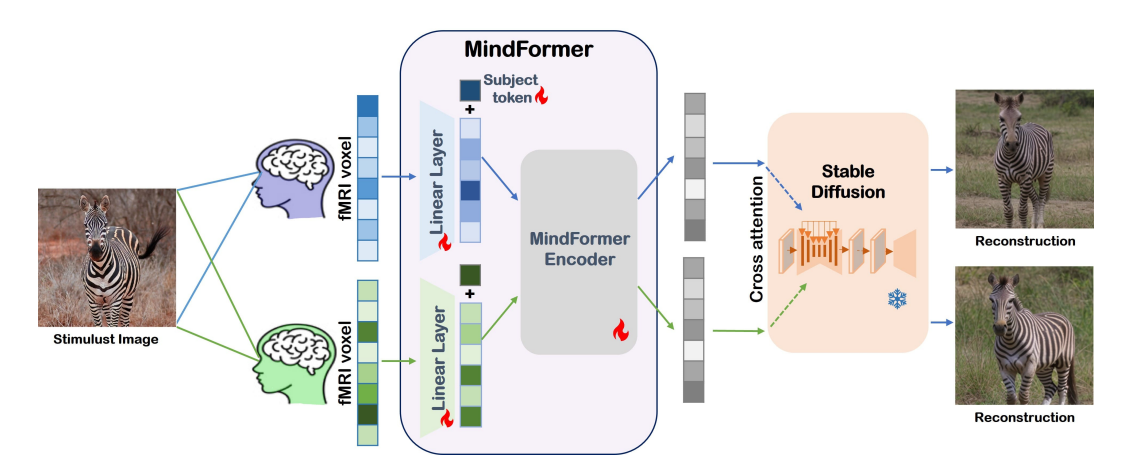


Figure 1: **MindFormer architecture**. The fMRI voxels obtained from observing the stimulus image are processed through the MindFormer to extract image features. These features are then utilized in conjunction with the Stable Diffusion model and a decoder to reconstruct the previously viewed image. The MindFormer is capable of distinguishing the origin of the information by using a learnable subject token, which allows it to identify from which specific subject the data was obtained.

the Stable Diffusion model, enhancing the decoding accuracy and reliability. Unlike previous studies that utilized CLIP embeddings, our semantic embedding via the IP-adapter is considerably smaller, reducing both computational costs and the risk of overfitting. Moreover, to synergistically combine training data from multiple subjects while accounting for individual differences, we introduce a subject-specific linear layer and the learnable subject token as inputs in the Transformer prompt. These subject specific components allow for the reconstruction of high-quality images from limited data sets by leveraging collective information from multiple subjects, improving its practical applicability in scenarios where data availability is restricted. Experimental results showed that our method maintains strong performance even with a limited amount of data by effectively leveraging the available common information across subjects to maximize accuracy and reliability.

Our contributions can be summarized as follows:

- We developed a unified model called MindFormer, designed to generate semantically meaningful condition embedding modules for the Stable Diffusion model, specifically tailored for multi-subject brain decoding from fMRI signals.
- MindFormer is a Transformer model that reduces dimensionality to decrease computational costs and minimize the risk of overfitting. Unlike previous methods that map brain signals into large CLIP image and text embeddings with dimensions of 257×768 and 77×768 respectively, MindFormer employs the IP-adapter to convert brain voxels into a compact 16x768-dimensional space. Additionally, it accounts for individual subject differences using a lightweight, subject-specific linear layer and learnable subject token, which significantly reduce the model's size. These enhancements make MindFormer considerably more efficient than existing models.
- To validate our method, we conducted experiments using the publicly available NSD dataset [17]. We utilized a subset of 982 images that were commonly viewed by all four subjects as the test set. The training set consisted of 8,859 images, with low overlap between subjects. Experimental results confirm that the proposed method achieves excellent performance in multi-subject brain decoding.

### 2 Related Works

### 2.1 fMRI-to-Image Reconstruction Models

The fMRI-to-Image reconstruction models are the advanced approaches that aim to translate brain activity, captured through functional magnetic resonance imaging (fMRI), into visual images. These

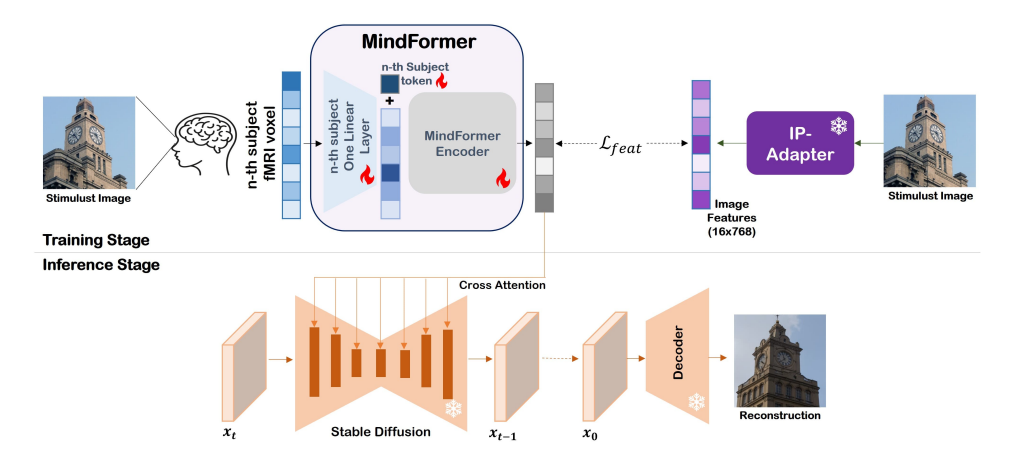


Figure 2: **Training stage**: The fMRI signals obtained after the n-th subject views an image are passed through a subject-specific linear layer. Subsequently, each signal is prepended with a learnable subject token and passed through the MindFormer Encoder. All subjects' signals are processed through the same MindFormer Encoder. The resulting embeddings are then trained to match the image feature embeddings obtained from passing the images through the IP-Adapter. **Inference Stage**: These obtained embeddings are integrated into the stable diffusion process. The diffusion model utilizes these embeddings to iteratively denoise and reconstruct the image. The embeddings trained to match those generated by the IP-Adapter enhance the model's ability to produce high-fidelity images that closely resemble the stimulus image.

models learn complex mappings between neural signals and visual representations, enabling the generation of images that closely resemble the original stimuli perceived by the subjects. Since the advent of deep learning, the models leverages the deep learning frameworks, to interpret and reconstruct the visual experiences of subjects based on their neural activity patterns. The advancements have integrated generative models, such as Generative Adversarial Networks (GANs) [13–16] and Variational Autoencoders (VAEs) [27], with fMRI data to improve the accuracy and quality of the reconstructed images. Seeliger et al. [16] explored the use of GANs for fMRI-to-image synthesis. Han et al. [27] demonstrated the effectiveness of VAEs in reconstructing visual stimuli from brain activity. Advancements in deep learning have enabled the generation of not only natural scenes but also human faces [28, 12] and video stimuli [29]. Moreover, advanced techniques like contrastive learning [30, 31] have been employed to align neural embeddings with visual embeddings more effectively. This alignment enhances the fidelity of the reconstructed images, ensuring that the generated visuals reflect the subjects' visual experiences.

#### 2.2 Image Generation Diffusion Model

Another notable innovation in the field of brain decoding is the use of diffusion models. Diffusion models have gained popularity in generative modeling due to their capability to convert a noise vector into an output image via a reverse diffusion process [32–34]. Recent studies [35, 36] have shown that diffusion models achieve superior image generation quality compared to GANs [37, 38], further solidifying their importance in this field. These models have been particularly influential in advancing brain decoding, offering enhanced flexibility and precision in capturing the nuances of visual experiences encoded in brain activity [18–24]. In most brain decoding studies that utilize diffusion models, researchers typically employ Stable Diffusion [39] or Versatile Diffusion [40] model. While Stable diffusion focuses on generating high-quality images by refining noise into coherent visuals, Versatile Diffusion facilitate substantial image variation, enabling tasks like style transfer. However, in Versatile Diffusion model, this variability can introduce challenges in brain decoding, as the reconstructed images may exhibit inconsistencies and artifacts. These discrepancies can complicate the accurate interpretation of neural activity, potentially reducing the fidelity of brain decoding outcomes.

Recent advancements in controllable image generation, such as ControlNet [41] and T2I-adapter [42], have shown that additional networks can guide image generation by plugging into existing text-to-image diffusion models. However, these methods often fall short in faithfully reproducing the reference image, primarily due to limitations in the cross-attention modules that inadequately

merge image and text features. IP-Adapter [26] addresses this issue by effectively integrating image features, enabling more accurate and detailed image generation based on reference inputs.

#### 3 The MindFormer

#### 3.1 Model Architecture

As shown in Fig. 1, the fMRI signals obtained after the *n*-th subject views an image are initially passed through a subject-specific linear layer. Following this, each signal is prepended with a unique learnable subject token and then processed through the MindFormer encoder. It is important to note that all subjects' signals are processed through the same instance of the MindFormer encoder, ensuring a unified encoding process. The embeddings produced from this process are subsequently trained to match the image feature embeddings obtained when the images are passed through the IP-Adapter.

The central concept of the IP-Adapter revolves around its innovative decoupled cross-attention mechanism. Instead of employing a single cross-attention layer to handle both text and image features simultaneously, the IP-Adapter introduces a dedicated cross-attention layer specifically for image features. This separation enables the model to focus on learning more detailed and image-specific features, enhancing its ability to capture the unique characteristics of visual data. This training ensures that the neural representations align closely with the visual features embeddings of IP-Adapter, facilitating accurate and reliable image reconstruction from the fMRI signals. Consequently, the trained embedding, from the brain signal, are integrated into the Stable Diffusion process. The diffusion model utilizes these embeddings to iteratively denoise and reconstruct the image to generate semantically aligned images.

Specifically, as shown in Fig. 2, MindFormer comprises of the subject specific linear layer and a single transformer encoder that incorporates unique learnable subject token. The architecture of MindFormer encoder follows the Vision Transformer (ViT) [43] encoder. Note that fMRI signals vary in size across subjects, primarily due to inherent differences in brain size and structure. To address the differing input voxel sizes, MindFormer maps each subject's voxels  $v^s$  into a uniform dimension of  $16\times768$  through individual linear layers  $\mathcal{E}_s$  for each subject s. Then, in the position of BERT [44] and ViT [43]'s [Class] token, we prepend a learnable embedding token  $x_{subj}$  to the output  $x^s = \mathcal{E}_s(v^s)$  of linear mapping. Addition use of learnable subject token ensures that the model accurately interprets and processes the neural data corresponding to multiple subject as well as each individual subject. Then, the position embeddings P are incorporated into the prepared embeddings to preserve positional information. The following steps proceed similarly to the transformer encoder in ViT. The Transformer encoder is composed of alternating layers of multi-headed self-attention (MSA) and MLP blocks. Layer normalization (LN) is applied before each block, with residual connections following each block. The MLP consists of two layers with a GELU activation function.

#### 3.2 Training Objectives

Formally, we represent the 1D fMRI voxels from subject s as  $v^s \in \mathbb{R}^{F_s}$ , where  $F_s$  denotes the subject specific size of the fMRI voxels. The corresponding image stimulus I can be extracted as image feature embeddings  $\boldsymbol{E}_I = [\boldsymbol{e}_1, \cdots, \boldsymbol{e}_N] \in \mathbb{R}^{d \times N}$  using a pretrained IP-Adapter with N=16 and d=768. Additionally, MindFormer maps the brain voxels  $\boldsymbol{v}^s$  into a  $16 \times 768$ -dimensional vector  $\boldsymbol{Z} = [\boldsymbol{z}_1, \cdots, \boldsymbol{z}_N]$ , matching the dimension of the image feature embeddings  $\boldsymbol{E}_I$  from the IP-Adapter [26]. Then, MindFormer is trained with feature domain  $l_1$ -loss and contrastive learning loss between fMRI and Images:

$$\mathcal{L}_{feat} = \mathcal{L}_1 + \alpha \cdot \mathcal{L}_{contrastive} \tag{1}$$

where  $\alpha > 0$  is a weight parameter. Specifically, the image feature-domain  $l_1$  loss measures how MindFormer can predict the image feature  $E_I$  from IP-Adapter:

$$\mathcal{L}_{1}(\boldsymbol{Z}, \boldsymbol{E}_{I}) = \frac{1}{N} \sum_{i=1}^{N} \|\boldsymbol{z}_{i} - \boldsymbol{e}_{i}\|_{1}$$
(2)

The contrast loss imposes the structural similarity between the MindFormer's output and that of IP-Adapter by increasing the similarity between the feature at the same location while decreasing the



Figure 3: **Natural scene and reconstructed image from human brain activity.** All reconstructions are outputs from MindFormer. Additional reconstruction samples can be found in Figure 4 and Appendix A.2.

similarity at different loations:

$$\mathcal{L}_{contrastive}(\boldsymbol{Z}, \boldsymbol{E}_{I}) = \frac{1}{N} \sum_{i=1}^{N} \left( \log \frac{e^{\boldsymbol{z}_{i} \cdot \boldsymbol{e}_{i}}}{\sum_{j=1}^{N} e^{\boldsymbol{z}_{i} \cdot \boldsymbol{e}_{j}}} \right)$$
(3)

### 4 Experiments

### 4.1 Experimental Results

**Experiment Settings.** The proposed model is implemented in PyTorch. The single subject model is trained on one NVIDIA RTX 3090 GPU with a 24GB memory, and the multi subject model is trained on one NVIDIA RTX V100 with a 32GB memorys. Across all experiments, the batch size is set to 4 per GPU and the epoch size is 50. The learning rate was set as  $3 \times 10^{-4}$ , and the moment parameters of the AdamW optimization algorithm [45] were set as  $\beta_1 = 0.9$ ,  $\beta_2 = 0.999$ .

**Dataset.** To better understand the task at hand, we illustrate the data used in our study. For all experiments, we used the widely-adopted Natural Scenes Dataset (NSD) [17], a public fMRI dataset containing high-resolution 7-Tesla fMRI scans of brain responses from eight healthy adult subjects viewing natural scenes from the MS-COCO dataset [46]. Following common practices [20–23, 25], our research primarily uses data from four subjects (subj01, 02, 05, 07) who completed all scan sessions. Specifically, only a subset of data—982 images—was commonly viewed by all four subjects and used as the test set. The remaining data, comprising 8,859 distinct images viewed by each subject, were used as the training set, resulting in 24,980 training samples without averaging across repetitions, similar to the method used by previous research. We utilize the dataset, preprocessed by [22], which consists of flattened fMRI voxels within the brain volume space corresponding to the "nsdgeneral" brain region. This region, defined by the authors of [17], includes the subset of voxels that are most responsive to visual stimuli.

**Results.** To quantitatively compare with other methods, we utilize eight image quality evaluation metrics as outlined in [21]. For assessing low-level properties, we use PixCorr, SSIM [47], AlexNet(2), and AlexNet(5) [48]. For evaluating higher-level properties, the metrics of Inception [49], CLIP [31], EffNet-B [50], and SwAV [51] are employed.

Figure 3 demonstrates MindFormer's strong performance across all four subjects, consistently producing accurate and reliable results. From the images, the effectiveness of the model is evidenced by its ability to generalize well and maintain high accuracy in decoding brain activity into visual images for each subject. The reconstructed images, shown in Figure 4, clearly illustrate the superior performance of our approach compared to existing methods. The results from the proposed method

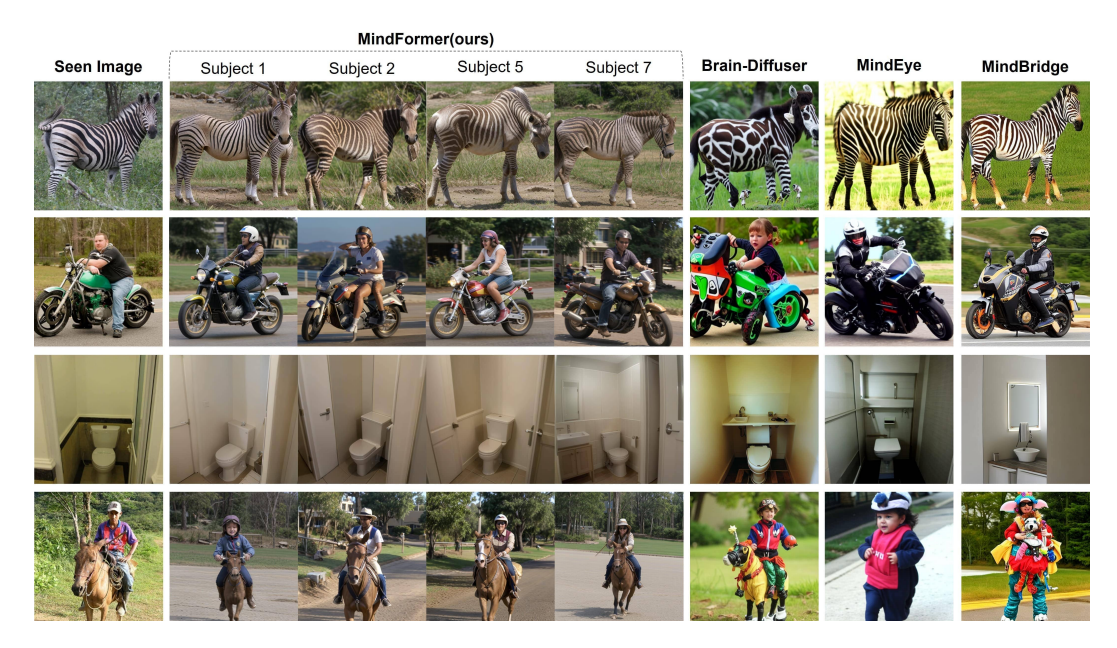


Figure 4: Visual comparison of our proposed MindFormer with other methods. Our resulting images are semantically closest to the seen images.

Method	# Models	Low-level				High-level			
		PixCorr ↑	SSIM ↑	Alex(2)↑	Alex(5)↑	Incep ↑	CLIP↑	EffNet-B↓	SwAV ↓
Takagi et al. [23]	4	_	_	83.0%	83.0%	76.0%	77.0%	_	_
Brain-Diffuser [21]	4	.254	.356	94.2%	96.2%	87.2%	91.5%	.775	.423
MindEye [22]	4	.309	.323	94.7%	97.8%	93.8%	94.1%	.645	.367
MindBridge (Single-) [25]	4	.148	.259	86.9%	95.3%	92.2%	94.3%	.713	.413
Ours (Single-)	4	.241	.352	93.5%	97.5%	93.5%	93.6%	.659	<u>.356</u>
MindBridge [25]	1	.151	.263	87.7%	95.5%	92.4%	94.7%	.712	.418
Ours (Multi-)	1	.243	.345	93.5%	<u>97.6%</u>	94.4%	<u>94.4</u> %	<u>.648</u>	.350

Table 1: Quantitative comparison of MindFormer's decoding performance against other models. **Bold**: best, <u>underline</u>: second best. The metrics presented are averaged across the data from 4 subjects. Unlike other methods, which generally require a separate model for each subject, our approach and MindBridge consolidate the process into one model. Among them, our approach achieved superior results in all metrics except for the CLIP score.

highlights the accuracy and fidelity of the visual outputs generated by our model, aligning closely with the original stimuli. In particular, our model's results demonstrate a high degree of semantic similarity to the stimulus images. This is evident in the ability of our model to accurately capture and reproduce the high-level features present in the original stimuli, resulting in reconstructed images that closely resemble the meaning and content of the stimulus images. This high semantic fidelity highlights the effectiveness of our approach in maintaining the integrity of the visual information during the decoding process.

Also, the quantitative metrics presented in Table 1 further support these findings, indicating significant improvements in high-level indicators such as Inception, CLIP, EffNet-B and SwAV. In brain decoding, low-level metrics evaluate the pixel-wise and structural similarity between original and reconstructed images. High-level metrics assess the semantic similarity and how well the reconstructed images capture the meaning and content of the originals. High-level metrics being high indicates that the model effectively captures and reconstructs the complex, abstract features of the stimulus, leading to more meaningful and contextually accurate representations. These results underscore the effectiveness of our model in accurately decoding and reconstructing visual experiences from neural data, thereby validating our approach and its contributions to the field. Not only does our model achieve high scores on high-level metrics, but it also consistently outperforms other models trained on data from multiple subjects, such as MindBridge, as demonstrated in Table 1. This table illustrates that our model attains superior scores across a range of metrics when compared to MindBridge, which is also designed to handle data from multiple subjects within a single model. These results suggest that

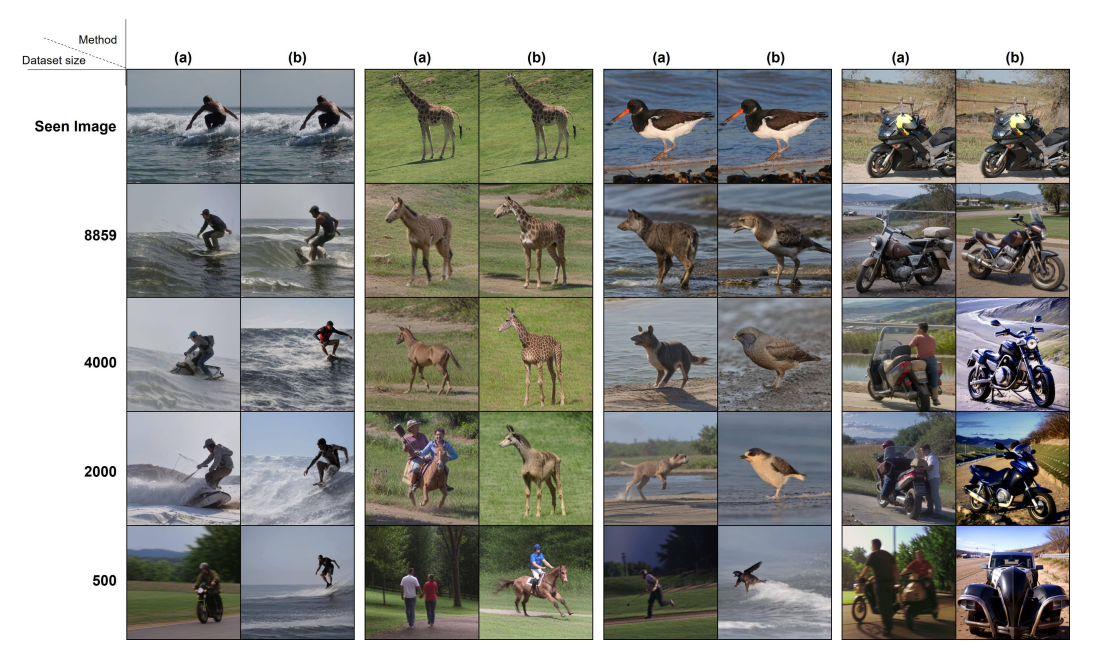


Figure 5: Performance comparison on limited datasets. The results shown are for Subject 1, evaluated on different dataset sizes: the entire dataset, 4000 samples, 2000 samples, and 500 samples. Two scenarios are compared: (a) single MindFormer scenario, where the MindFormer is trained exclusively on subject 1's data, and (b) multi MindFormer scenario, where the MindFormer is trained on data from Subjects 1, 2, 5, and 7.

Method # Dataset		Low-level				High-level			
method " Dutuset	" Daniset	PixCorr ↑	SSIM ↑	Alex(2)↑	Alex(5)↑	Incep↑	CLIP↑	EffNet-B↓	SwAV↓
(a)	500	.160	.308	80.8%	87.5%	77.5%	78.2%	.854	.499
(b)	500	.179	.351	87.7%	93.0%	85.5%	85.5%	.796	.461
(a)	2000	.221	.344	90.6%	95.6%	88.6%	89.1%	.757	.401
(b)	2000	.241	.352	92.4%	96.8%	91.5%	92.1%	.719	.409
(a)	4000	.264	.369	93.5%	96.9%	91.6%	92.3%	.701	.374
(b)	4000	.227	.327	93.0%	97.5%	93.6%	93.7%	.680	.392
(a)	all	.270	.356	95.2%	98.0%	93.4%	93.6%	.660	.354
(b)	all	.271	.351	95.3%	98.2%	95.1%	94.7%	.641	.339

Table 2: Quantitative comparison of the limited dataset size. The above results are from Subject 1. **Bold**: best. Two scenarios are compared: (a) single MindFormer scenario, where the MindFormer is trained exclusively on subject 1's data, and (b) multi MindFormer scenario, where the MindFormer is trained on data from Subjects 1, 2, 5, and 7.

our model is more effective in multi-subject brain decoding tasks, thereby implying its potential for broader adoption and application in the field. By excelling in both high-level semantic representation and overall performance, our model demonstrates a significant advancement in the ability to decode and reconstruct brain activity from multiple individuals within a unified framework.

#### 4.2 Ablation Study

**Exploiting multiple subject data set.** Given the limited training data, obtaining a sufficiently large fMRI dataset from new subjects is a challenging task. Therefore, it is crucial to achieve high-quality result images even with a small amount of data. To investigate this, we perform ablation study using single MindFormer and multi MindFormer experimental setups. In single MindFormer scenario, MindFormer trains only the dataset of Subject 1. In multi MindFormer scenario, the training process includes not only subject 1 but also subjects 2, 5, and 7. Data from each of these subjects is processed through the MindFormer framework, allowing the model to learn from a varied set of neural patterns. This approach ensures that the model can generalize more effectively across different individuals,



Figure 6: Reconstructed image from human brain activity on the presence of learnable subject tokens (ST) in MindFormer. The model incorporating subject tokens demonstrates higher correlation in semantic meaning with the seen image.

Subject Token (ST)	Low-level				High-level			
~ <b>,</b> (~ - /	PixCorr ↑	SSIM $\uparrow$	Alex(2)↑	Alex(5)↑	Incep ↑	CLIP↑	EffNet-B $\downarrow$	SwAV $\downarrow$
without ST with ST	.233 <b>.243</b>	<b>.349</b> .345	92.8% <b>93.5%</b>	97.1% <b>97.6%</b>	93.4% <b>94.4</b> %	93.4% <b>94.4</b> %	.662 .648	.359 .351

Table 3: Quantitative comparison of results on the presence or absence of learnable subject tokens (ST). **Bold**: best. The inclusion of subject tokens significantly improved the model's accuracy, as evidenced by the higher scores across various evaluation metrics. This demonstrates that learnable subject tokens play a crucial role in enhancing the precision and reliability of the brain decoding process.

thereby enhancing its decoding accuracy and robustness. By incorporating multiple subjects, the MindFormer can leverage the collective information, leading to improved performance in brain decoding tasks.

Figure 5 and Table 2 presents the reconstructed images and metric results for subject 1 across different dataset sizes: the entire dataset, 4000 samples, 2000 samples, and 500 samples. Overall, the results indicate that the multi MindFormer approach consistently outperforms the single MindFormer. Notably, the results obtained using only 2000 samples demonstrate that multi MindFormer, which is our method, can effectively reconstruct high-quality images even with a limited amount of data. Although the performance degraded with 500 samples, multi MinFormer scenario still outperforms the single MindFormer. Specifically, Figure 5 shows that as the dataset size decreases, the single MindFormer struggles to preserve the semantic aspects of the stimulus image, whereas the multi MindFormer maintains this semantic fidelity well. This highlights the robustness and efficiency of multi MindFormer in leveraging small datasets to achieve superior image reconstruction.

Importance of subject tokens. Using learnable subject tokens in MindFormer has several positive effects. First, it allows the model to accurately distinguish between inputs from different subjects, ensuring that individual-specific neural patterns are correctly interpreted and processed. This enhances the precision of brain decoding by aligning the model's understanding with the unique characteristics of each subject's brain activity. Additionally, the incorporation of learnable subject tokens improves the model's ability to generalize across multiple subjects, as it can adapt to variability in neural signals while maintaining high performance in decoding tasks. Overall, subject tokens contribute to more reliable and robust decoding outcomes, facilitating better insights into neural representations. Figure 6 and Table 3 provides evidence for these benefits by showing superior performance results when subject tokens are used. Also, by using subject tokens, this unified model approach offers significant advantages in terms of efficiency and scalability, allowing for comprehensive analysis and image reconstruction across different individuals without the need for multiple models.

### 5 Discussion

The results from our experiments show the efficacy and robustness of the MindFormer model in cross-subject brain decoding. One of the key findings is the significant improvement in image reconstruction accuracy when incorporating subject tokens and utilizing a multi-subject training approach. Notably, even with a limited dataset, the MindFormer demonstrates its capability to reconstruct high-quality images, outperforming models trained on larger datasets. This is particularly important given the challenges associated with obtaining large fMRI datasets from new subjects. The ability to achieve good performance with smaller datasets not only validates the efficiency of the MindFormer but also points to its practical applicability in real-world scenarios where data availability may be constrained. Moreover, the comparison between single-subject and multi-subject training

further validates the advantage of leveraging data from multiple subjects. The results consistently indicate that the MindFormer approach, which integrates data from subjects 2, 5, and 7 along with subject 1, yields better performance metrics. This suggests that the model benefits from the additional information provided by the diverse set of neural patterns, enhancing its generalization capabilities and robustness.

Although the MindBridge model [25] is designed to exploit multi-subject fMRI data for training, it relies on an aggregation function to reduce dimensionality, leading to information loss and lower performance. On the other hand, the learnable subject tokens play a pivotal role in our MindFormer framework. By allowing the model to differentiate between neural signals from different subjects, the subject tokens ensure that the individual-specific nuances in brain activity are preserved and accurately decoded. Table 3 demonstrates the performance improvements attributed to the use of subject tokens, highlighting their importance in achieving high-fidelity decoding outcomes. This approach also streamlines the process by enabling the use of a single unified model for multiple subjects, offering significant advantages in terms of efficiency and scalability.

### 6 Conclusion

In this paper, we proposed "MindFormer", a new transformer architecture for powerful multi-subject brain decoding framework when combined with Stable Diffusion model. The model successfully surpass the existing multi-subject brain decoding framework. The inclusion of learnable subject tokens contributed to the model's robustness, enabling it to generalize effectively across different subjects. The proposed method, MindFormer, successfully reconstructs images from fMRI signals with higher accuracy than previous models, thanks to its innovative use of the IP-Adapter and learnable subject tokens. Our contributions include the development of a unified model for multisubject brain decoding, the creation of a lightweight deep learning model, and the demonstration of strong performance with limited data. Overall, MindFormer provides a new framework for understanding multi-subject brain decoding and common neural patterns. The model's ability to leverage shared information across subjects while maintaining individual-specific accuracy marks a significant advancement in the field of brain decoding.

Limitation However, there are several limitations to our approach that must be addressed in future research. First, the current implementation of MindFormer primarily focuses on visual stimuli. Extending this approach to decode more complex cognitive and sensory experiences will require substantial advancements in both model architecture and training methodologies. Another limitation is the computational complexity associated with training much more subjects. Although our approach reduces the parameter count compared to existing models, training these models with over about 10 subjects still require significant computational resources. Future work should aim to optimize the model further to make it more accessible and feasible for broader applications. That said, the small model size could impose limitations on the ability to decode brain activity at the individual subject level. Due to the reduced capacity of the model, it may struggle to capture the unique and complex neural patterns specific to each subject, thereby affecting the accuracy and effectiveness of the decoding process.

**Societal Impact** Ethical considerations, such as privacy and consent, are critical in this domain. The ethical implications of visual brain decoding, including privacy concerns and the potential for misuse, must be carefully considered. Collaborative efforts between neuroscientists, computer scientists, and ethicists will be essential in advancing this field responsibly and effectively. As visual brain decoding technologies continue to mature, they hold promise for profound impacts on neuroscience, clinical practice, and our understanding of the human.

### References

- [1] Mo Chen, Junwei Han, Xintao Hu, Xi Jiang, Lei Guo, and Tianming Liu. Survey of encoding and decoding of visual stimulus via fmri: an image analysis perspective. *Brain imaging and behavior*, 8:7–23, 2014.
- [2] Alexandre Défossez, Charlotte Caucheteux, Jérémy Rapin, Ori Kabeli, and Jean-Rémi King. Decoding speech perception from non-invasive brain recordings. *Nature Machine Intelligence*, 5(10):1097–1107, 2023.

- [3] Bing Du, Xiaomu Cheng, Yiping Duan, and Huansheng Ning. fmri brain decoding and its applications in brain-computer interface: A survey. *Brain Sciences*, 12(2):228, 2022.
- [4] Jacob S Prince, Ian Charest, Jan W Kurzawski, John A Pyles, Michael J Tarr, and Kendrick N Kay. Improving the accuracy of single-trial fmri response estimates using glmsingle. *Elife*, 11:e77599, 2022.
- [5] Rajesh PN Rao and Dana H Ballard. Predictive coding in the visual cortex: a functional interpretation of some extra-classical receptive-field effects. *Nature neuroscience*, 2(1):79–87, 1999.
- [6] Sanne Schoenmakers, Markus Barth, Tom Heskes, and Marcel Van Gerven. Linear reconstruction of perceived images from human brain activity. *NeuroImage*, 83:951–961, 2013.
- [7] Roman Beliy, Guy Gaziv, Assaf Hoogi, Francesca Strappini, Tal Golan, and Michal Irani. From voxels to pixels and back: Self-supervision in natural-image reconstruction from fmri. *Advances in Neural Information Processing Systems*, 32, 2019.
- [8] Guy Gaziv, Roman Beliy, Niv Granot, Assaf Hoogi, Francesca Strappini, Tal Golan, and Michal Irani. Self-supervised natural image reconstruction and large-scale semantic classification from brain activity. *NeuroImage*, 254:119121, 2022.
- [9] Zijin Gu, Keith Jamison, Amy Kuceyeski, and Mert Sabuncu. Decoding natural image stimuli from fmri data with a surface-based convolutional network. *arXiv preprint arXiv:2212.02409*, 2022.
- [10] Tomoyasu Horikawa and Yukiyasu Kamitani. Generic decoding of seen and imagined objects using hierarchical visual features. *Nature communications*, 8(1):15037, 2017.
- [11] Guohua Shen, Tomoyasu Horikawa, Kei Majima, and Yukiyasu Kamitani. Deep image reconstruction from human brain activity. *PLoS computational biology*, 15(1):e1006633, 2019.
- [12] Rufin VanRullen and Leila Reddy. Reconstructing faces from fmri patterns using deep generative neural networks. Communications biology, 2(1):193, 2019.
- [13] Sikun Lin, Thomas Sprague, and Ambuj K Singh. Mind reader: Reconstructing complex images from brain activities. *Advances in Neural Information Processing Systems*, 35:29624–29636, 2022.
- [14] Milad Mozafari, Leila Reddy, and Rufin VanRullen. Reconstructing natural scenes from fmri patterns using bigbigan. In 2020 International joint conference on neural networks (IJCNN), pages 1–8. IEEE, 2020.
- [15] Furkan Ozcelik, Bhavin Choksi, Milad Mozafari, Leila Reddy, and Rufin VanRullen. Reconstruction of perceived images from fmri patterns and semantic brain exploration using instance-conditioned gans. In 2022 International Joint Conference on Neural Networks (IJCNN), pages 1–8. IEEE, 2022.
- [16] Katja Seeliger, Umut Güçlü, Luca Ambrogioni, Yagmur Güçlütürk, and Marcel AJ Van Gerven. Generative adversarial networks for reconstructing natural images from brain activity. *NeuroImage*, 181:775–785, 2018.
- [17] Emily J Allen, Ghislain St-Yves, Yihan Wu, Jesse L Breedlove, Jacob S Prince, Logan T Dowdle, Matthias Nau, Brad Caron, Franco Pestilli, Ian Charest, et al. A massive 7t fmri dataset to bridge cognitive neuroscience and artificial intelligence. *Nature neuroscience*, 25(1):116–126, 2022.
- [18] Zijiao Chen, Jiaxin Qing, Tiange Xiang, Wan Lin Yue, and Juan Helen Zhou. Seeing beyond the brain: Conditional diffusion model with sparse masked modeling for vision decoding. In *Proceedings of the IEEE/CVF Conference on Computer Vision and Pattern Recognition*, pages 22710–22720, 2023.
- [19] Yizhuo Lu, Changde Du, Qiongyi Zhou, Dianpeng Wang, and Huiguang He. Minddiffuser: Controlled image reconstruction from human brain activity with semantic and structural diffusion. In *Proceedings of the 31st ACM International Conference on Multimedia*, pages 5899–5908, 2023.
- [20] Weijian Mai and Zhijun Zhang. Unibrain: Unify image reconstruction and captioning all in one diffusion model from human brain activity. *arXiv preprint arXiv:2308.07428*, 2023.
- [21] Furkan Ozcelik and Rufin VanRullen. Natural scene reconstruction from fmri signals using generative latent diffusion. *Scientific Reports*, 13(1):15666, 2023.
- [22] Paul Scotti, Atmadeep Banerjee, Jimmie Goode, Stepan Shabalin, Alex Nguyen, Aidan Dempster, Nathalie Verlinde, Elad Yundler, David Weisberg, Kenneth Norman, et al. Reconstructing the mind's eye: fmri-toimage with contrastive learning and diffusion priors. Advances in Neural Information Processing Systems, 36, 2024.

- [23] Yu Takagi and Shinji Nishimoto. High-resolution image reconstruction with latent diffusion models from human brain activity. In *Proceedings of the IEEE/CVF Conference on Computer Vision and Pattern Recognition*, pages 14453–14463, 2023.
- [24] Weihao Xia, Raoul de Charette, Cengiz Oztireli, and Jing-Hao Xue. Dream: Visual decoding from reversing human visual system. In Proceedings of the IEEE/CVF Winter Conference on Applications of Computer Vision, pages 8226–8235, 2024.
- [25] Shizun Wang, Songhua Liu, Zhenxiong Tan, and Xinchao Wang. Mindbridge: A cross-subject brain decoding framework. arXiv preprint arXiv:2404.07850, 2024.
- [26] Hu Ye, Jun Zhang, Sibo Liu, Xiao Han, and Wei Yang. Ip-adapter: Text compatible image prompt adapter for text-to-image diffusion models. arXiv preprint arXiv:2308.06721, 2023.
- [27] Kuan Han, Haiguang Wen, Junxing Shi, Kun-Han Lu, Yizhen Zhang, Di Fu, and Zhongming Liu. Variational autoencoder: An unsupervised model for encoding and decoding fmri activity in visual cortex. NeuroImage, 198:125–136, 2019.
- [28] Thirza Dado, Yağmur Güçlütürk, Luca Ambrogioni, Gabriëlle Ras, Sander Bosch, Marcel van Gerven, and Umut Güçlü. Hyperrealistic neural decoding for reconstructing faces from fmri activations via the gan latent space. *Scientific reports*, 12(1):141, 2022.
- [29] Chong Wang, Hongmei Yan, Wei Huang, Jiyi Li, Yuting Wang, Yun-Shuang Fan, Wei Sheng, Tao Liu, Rong Li, and Huafu Chen. Reconstructing rapid natural vision with fmri-conditional video generative adversarial network. *Cerebral Cortex*, 32(20):4502–4511, 2022.
- [30] Ting Chen, Simon Kornblith, Mohammad Norouzi, and Geoffrey Hinton. A simple framework for contrastive learning of visual representations. In *International conference on machine learning*, pages 1597–1607. PMLR, 2020.
- [31] Alec Radford, Jong Wook Kim, Chris Hallacy, Aditya Ramesh, Gabriel Goh, Sandhini Agarwal, Girish Sastry, Amanda Askell, Pamela Mishkin, Jack Clark, et al. Learning transferable visual models from natural language supervision. In *International conference on machine learning*, pages 8748–8763. PMLR, 2021.
- [32] Jonathan Ho, Ajay Jain, and Pieter Abbeel. Denoising diffusion probabilistic models. *Advances in neural information processing systems*, 33:6840–6851, 2020.
- [33] Alexander Quinn Nichol and Prafulla Dhariwal. Improved denoising diffusion probabilistic models. In *International conference on machine learning*, pages 8162–8171. PMLR, 2021.
- [34] Jiaming Song, Chenlin Meng, and Stefano Ermon. Denoising diffusion implicit models. *arXiv preprint arXiv:2010.02502*, 2020.
- [35] Prafulla Dhariwal and Alexander Nichol. Diffusion models beat gans on image synthesis. Advances in neural information processing systems, 34:8780–8794, 2021.
- [36] Yang Song, Jascha Sohl-Dickstein, Diederik P Kingma, Abhishek Kumar, Stefano Ermon, and Ben Poole. Score-based generative modeling through stochastic differential equations. arXiv preprint arXiv:2011.13456, 2020.
- [37] Andrew Brock, Jeff Donahue, and Karen Simonyan. Large scale gan training for high fidelity natural image synthesis. *arXiv preprint arXiv:1809.11096*, 2018.
- [38] Han Zhang, Ian Goodfellow, Dimitris Metaxas, and Augustus Odena. Self-attention generative adversarial networks. In *International conference on machine learning*, pages 7354–7363. PMLR, 2019.
- [39] Robin Rombach, Andreas Blattmann, Dominik Lorenz, Patrick Esser, and Björn Ommer. High-resolution image synthesis with latent diffusion models. In *Proceedings of the IEEE/CVF conference on computer* vision and pattern recognition, pages 10684–10695, 2022.
- [40] Xingqian Xu, Zhangyang Wang, Gong Zhang, Kai Wang, and Humphrey Shi. Versatile diffusion: Text, images and variations all in one diffusion model. In *Proceedings of the IEEE/CVF International Conference* on Computer Vision, pages 7754–7765, 2023.
- [41] Lvmin Zhang, Anyi Rao, and Maneesh Agrawala. Adding conditional control to text-to-image diffusion models. In *Proceedings of the IEEE/CVF International Conference on Computer Vision*, pages 3836–3847, 2023.

- [42] Chong Mou, Xintao Wang, Liangbin Xie, Yanze Wu, Jian Zhang, Zhongang Qi, and Ying Shan. T2i-adapter: Learning adapters to dig out more controllable ability for text-to-image diffusion models. In *Proceedings of the AAAI Conference on Artificial Intelligence*, volume 38, pages 4296–4304, 2024.
- [43] Alexey Dosovitskiy, Lucas Beyer, Alexander Kolesnikov, Dirk Weissenborn, Xiaohua Zhai, Thomas Unterthiner, Mostafa Dehghani, Matthias Minderer, Georg Heigold, Sylvain Gelly, et al. An image is worth 16x16 words: Transformers for image recognition at scale. *arXiv* preprint arXiv:2010.11929, 2020.
- [44] Jacob Devlin, Ming-Wei Chang, Kenton Lee, and Kristina Toutanova. Bert: Pre-training of deep bidirectional transformers for language understanding. *arXiv* preprint arXiv:1810.04805, 2018.
- [45] Ilya Loshchilov and Frank Hutter. Decoupled weight decay regularization. *arXiv preprint* arXiv:1711.05101, 2017.
- [46] Tsung-Yi Lin, Michael Maire, Serge Belongie, James Hays, Pietro Perona, Deva Ramanan, Piotr Dollár, and C Lawrence Zitnick. Microsoft coco: Common objects in context. In *Computer Vision–ECCV 2014: 13th European Conference, Zurich, Switzerland, September 6-12, 2014, Proceedings, Part V 13*, pages 740–755. Springer, 2014.
- [47] Zhou Wang, Alan C Bovik, Hamid R Sheikh, and Eero P Simoncelli. Image quality assessment: from error visibility to structural similarity. *IEEE transactions on image processing*, 13(4):600–612, 2004.
- [48] Alex Krizhevsky, Ilya Sutskever, and Geoffrey E Hinton. Imagenet classification with deep convolutional neural networks. *Advances in neural information processing systems*, 25, 2012.
- [49] Christian Szegedy, Vincent Vanhoucke, Sergey Ioffe, Jon Shlens, and Zbigniew Wojna. Rethinking the inception architecture for computer vision. In *Proceedings of the IEEE conference on computer vision and* pattern recognition, pages 2818–2826, 2016.
- [50] Mingxing Tan and Quoc Le. Efficientnet: Rethinking model scaling for convolutional neural networks. In *International conference on machine learning*, pages 6105–6114. PMLR, 2019.
- [51] Mathilde Caron, Ishan Misra, Julien Mairal, Priya Goyal, Piotr Bojanowski, and Armand Joulin. Unsupervised learning of visual features by contrasting cluster assignments. Advances in neural information processing systems, 33:9912–9924, 2020.

## A Appendix

### A.1 Comparison of Model Parameter Number

Method	The number of model parameter					
Brain-Diffuser	Low Level High Level	1,433,616,800 12,076,800				
MindEye	Low Level High Level	205,505,988 1,003,635,072				
MindBridge	single (for 1 subject) multi (for 4 subjects)	561,283,712 693,579,264				
MindFormer	single (for 1 subject) multi (for 4 subjects)	304,782,336 765,607,680				

Table 4: MindBridge and MindFormer have fewer parameters compared to other models. In particular, the single-MindFormer for one subject has the fewest number of parameters among them. Using models with fewer parameters is a way to reduce computational costs.

#### A.2 Additional Results of multi MindFormer Model

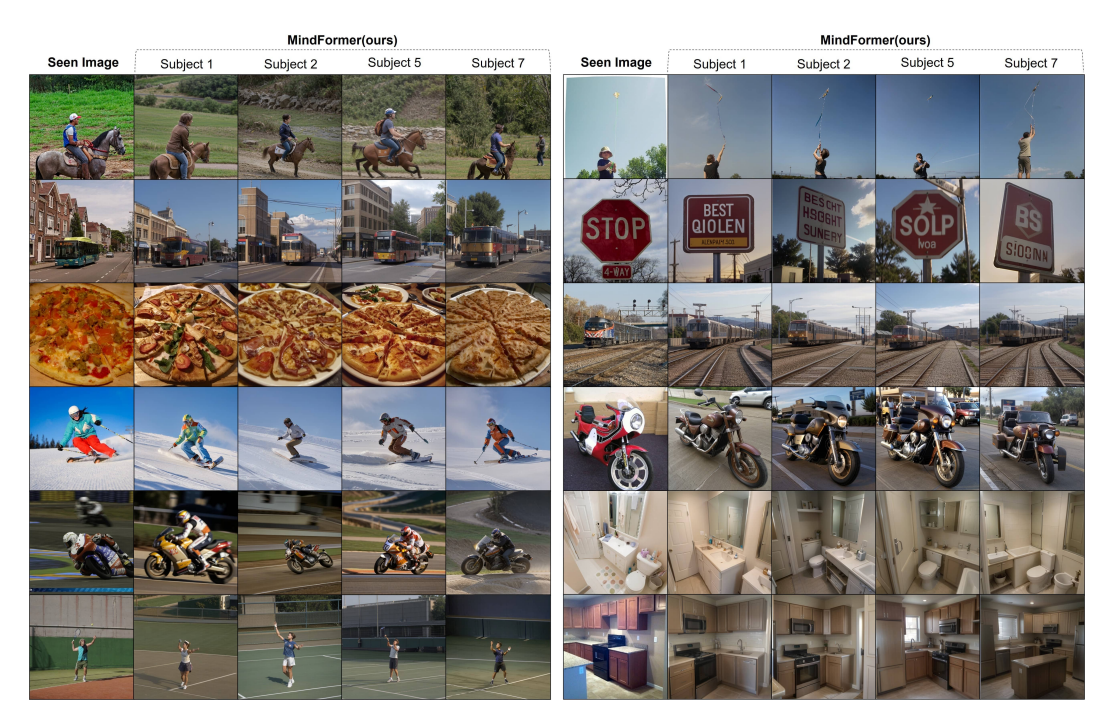


Figure 7: Additional reconstructed image from human brain activity. All reconstructions are outputs from the our one integrated model, MindFormer.

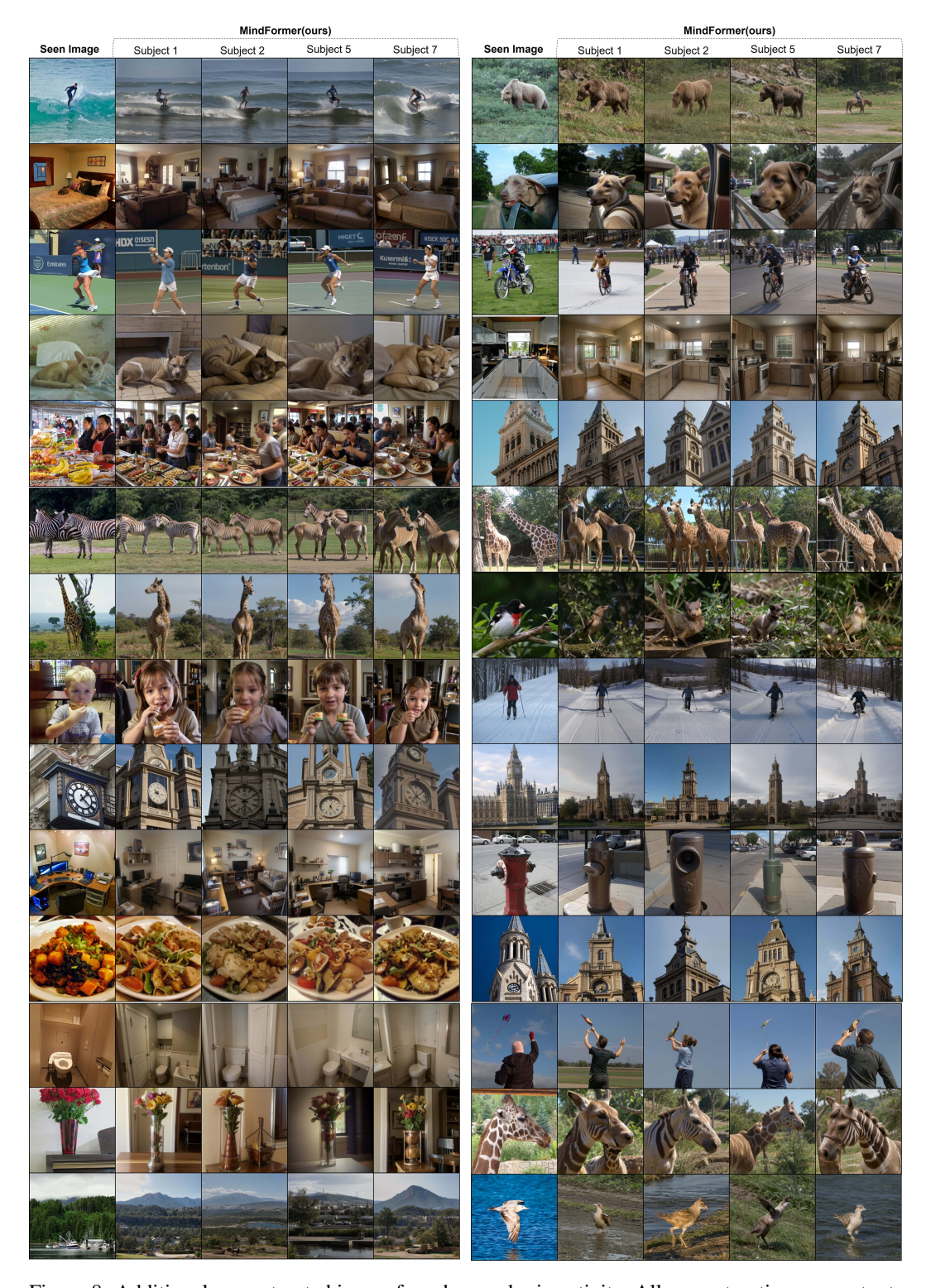


Figure 8: Additional reconstructed image from human brain activity. All reconstructions are outputs from the our one integrated model, MindFormer.